SolarPACES 2024, 30th International Conference on Concentrating Solar Power, Thermal, and Chemical Energy Systems

Solar Industrial Process Heat and Thermal Desalination

https://doi.org/10.52825/solarpaces.v3i.2446

© Authors. This work is licensed under a Creative Commons Attribution 4.0 International License

Published: 23 Oct. 2025

Numerical Modelling of a Solar Thermochemical Heat Transformer for Industrial Heating Applications

Ramin Roushenas¹, Marco Ballatore¹, Artem Sybir², Aldo Cosquillo³, Marc Linder³, and Abhishek K. Singh^{1,*}

¹Department of Thermal and Fluid Engineering, University of Twente, 7500 AE Enschede, the Netherlands ²TMEC; 49005, Dnipro, Dmytro Yavornytskyi Ave. 2a, 31, Ukraine

³Institute of Engineering Thermodynamics, German Aerospace Center (DLR); Pfaffenwaldring 38-40 70569 Stuttgart, Germany

*Correspondence: Abhishek K. Singh, a.k.singh@utwente.nl

Abstract. Replacing fossil fuel-based industrial heating systems with sustainable alternatives such as solar thermal systems is necessary for achieving sustainable development goals. Often low-concentrated solar collectors are cheaper yet their low-temperature output limits their applications in the industry. The thermochemical heat transformers can be integrated with these collectors to achieve an upgraded output temperature without electricity consumption. Furthermore, these thermochemical systems have an inherent capability of heat storage in chemical bonds thereby mitigating the intermittency issue of solar energy sources. In this research, an innovative packed-bed thermochemical reactor in a closed system configuration is introduced and simulated numerically. The main objective of this analysis is to scrutinize how well the proposed design operates in terms of heat and mass transfer. In this reactor, SrBr₂ hydrate is used as the thermochemical material. The study indicates that the proposed design can potentially upgrade the temperature by 100 °C and maintain it at 300 °C for about 40 minutes. This modular design, which can be scaled up easily for large applications, predicts the full conversion of reactions and shows a flexible temperature boost of low-concentrated collectors output.

Keywords: Thermochemical Heat Upgrade, Numerical Modelling, Salt Hydrate

1. Introduction

The climate change due to burning fossil fuels, specifically over recent decades, has turned attention toward utilizing renewable sources such as solar and wind [1]. Solar thermal collectors, as a potential pathway for cleaner heat production, can be a viable alternative to supply medium-to-high temperature industrial heat provided they are cost-effective and integrate a storage system to mitigate the intermittency issue of solar radiation. Thermochemical heat upgrade (TCHU) systems are uniquely situated to tackle these issues because they can boost the low-temperature heat from a cheaper, low-concentrated solar collector or any other source without consuming any electricity and have an inherent capability of storing heat in chemical bonds, making them a low-cost and reliable industrial heating solution.

Applying numerical modelling is an indispensable part of understanding a system in order to predict its behaviour under different scenarios. Indeed, experimental analysis along with simulations leads to optimum outcomes. Stengler et al. [2] evaluated thermal upgrade of a 1

kW thermochemical energy storage using SrBr₂/ SrBr₂.H₂O as heat storage material. This investigation took both experimental and numerical analysis into account to obtain a better understanding of effective parameters on thermal power. Comparing heat versus mass transfer, it was identified that heat transfer plays a key role in the overall thermal performance. Jinjin et al. [3] explored a new design for thermochemical energy storage based on numerical analysis. The salt hydrate of hexahydrate/monohydrate strontium bromide was used as the reactive material and the research focus was to enhance heat and mass transfer and reduces the likelihood of salt liquefaction. The main findings highlight a 26% reduction in reaction time and a 2.5% rise in thermal efficiency. Another simulation [4] worked on topology optimization of a closed thermochemical reactor working based on SrBr₂/ SrBr₂.H₂O. They introduced a new framework for optimizing fins structures and achieved an advancement in performance by up to 3 times.

The focus of this study is to investigate the performance of an innovative thermochemical reactor design. The structure is based on a plate-type heat exchanger whose modular design can be scaled up for large applications easily. In this study, a numerical model considering heat and mass transfer coupled with thermochemical material kinetics is developed for the proposed design. This system can be employed for heat upgrade of low-temperature applications such as solar thermal collectors up to 300 °C and higher.

2. System Description

Figure 1 schematically illustrates the operation of the system. The introduced packed-bed thermochemical heat upgrade operates in a closed configuration in which the reactive gas (pure water vapor) is circulated in a closed loop. Therefore, there is the opportunity to pressurize the reactive gas inside the evaporator by utilizing waste heat and without consuming electricity for compression. Over the dehydration phase, the thermochemical material absorbs heat from heat transfer fluid (HTF) and undergoes an endothermic reaction. The water molecules leave the salt particles and move toward the condenser; so, their recombination is prevented. Subsequently, the consumed energy is stored in the form of chemical potential. During discharging phase, the condensed water vapor is evaporated, and finally injected into the second reactor. The salt crystals are hydrated as they come into contact with water vapor and release the stored heat which is absorbed indirectly by heat transfer fluid. The steam pressure supplied in the hydration reactor acts as the driving force for the heat upgrade. As the steam pressure increases, the hydration temperature also rises. This relationship is shown in Figure 2 which demonstrates experimental equilibrium lines [5] and the theoretical equilibrium based on the Van't Hoff equation for anhydrous/monohydrate SrBr₂ reactions.

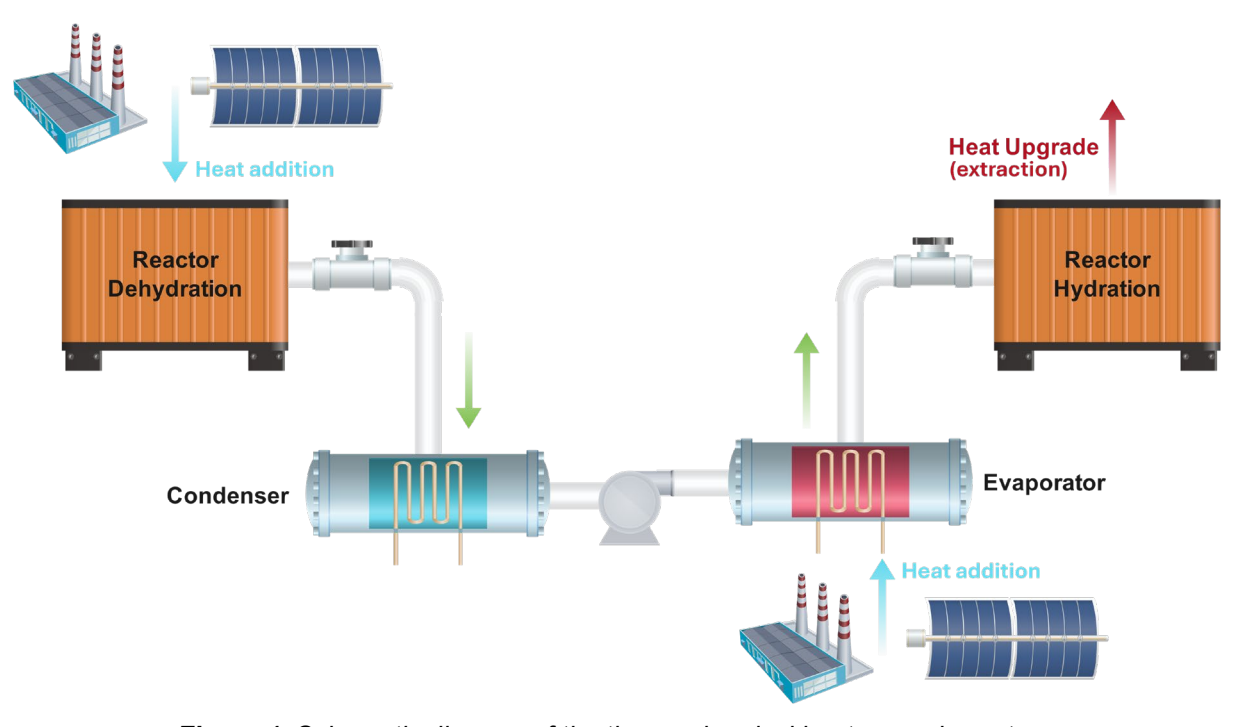


Figure 1. Schematic diagram of the thermochemical heat upgrade system.

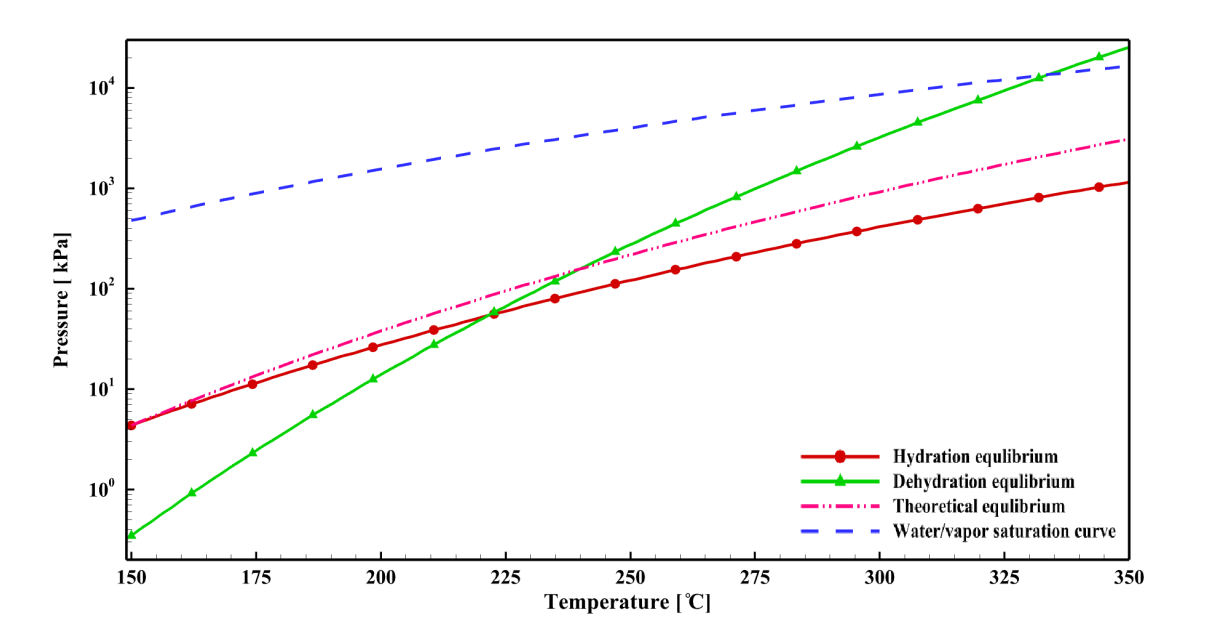


Figure 2. P-T diagram of the SrBr₂ and water.

Figure 3 presents the domains in 3D (left) and schematically in 2D (right) ignoring pipes, connections, and other equipment. Due to the nature of the design, the streams of steam and HTF are co-current for dehydration and counter-current for hydration reactions. Here, the water vapor channel (1), fiberglass (2), material (3), heat exchanger plate (4), and HTF (5) are shown. Their thickness are respectively 2 mm, 1 mm, 10 mm, 3 mm, and 6 mm. Also, each domain has a length of 170 mm and a width of 107 mm. The reactor is connected to the condenser/evaporator through a 55 mm width channel.

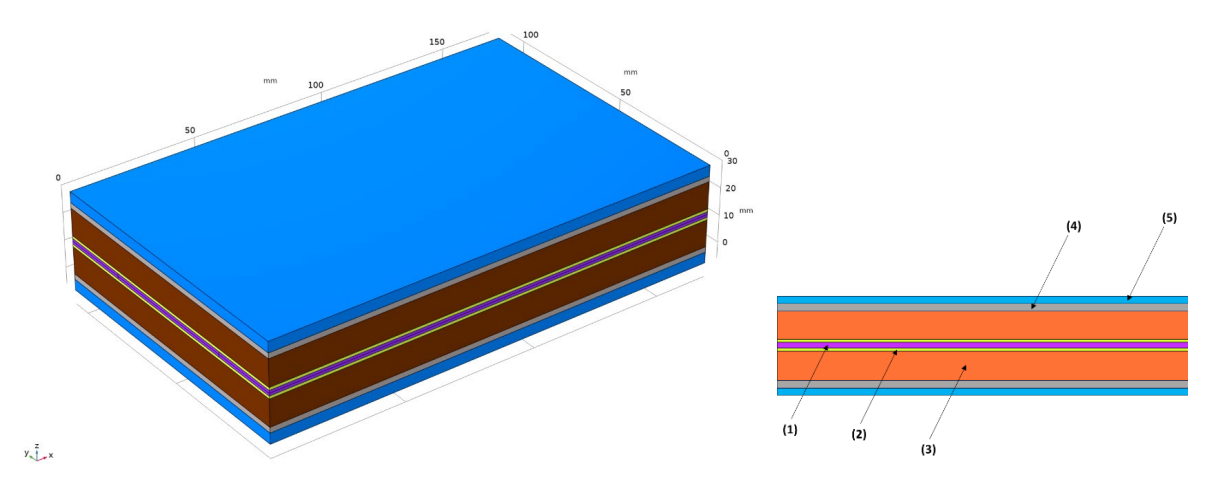


Figure 3. Reactor domains for numerical modelling.

3. Modelling

To determine the performance of the proposed reactor design, a detailed numerical model of the thermochemical heat upgrade reactor is developed. The reactor is modelled based on Finite Element Method (FEM) via COMSOL Multiphysics software. Given the symmetrical boundary for the reactor shown in Figure 3, one layer was implemented for transient simulations. Taking several criteria into account, such as reaction kinetics, operating temperature range, non-toxicity, reversibility, cyclability, etc. led to the selection of anhydrous/monohydrate SrBr₂ as the best reactive material candidate for the proposed TCHT. Water vapor desorption/ adsorption of this salt hydrate is given as:

$$SrBr_2 \cdot H_2O_{(s)} + \Delta H \rightleftharpoons SrBr_{2(s)} + H_2O_{(g)}; \ \Delta H = 71.98 \, kJ/mol$$
 (1)

3.1 Assumptions

The following main assumptions are made for modelling:

- The reactor is perfectly isolated, so no heat or mass transfer occurs with the environment.
- Energy conservation for porous mediums is modelled based on local thermal equilibrium
- Since the operation is at low temperatures, the radiation heat transfer is negligible; thus, the primary methods by which the thermal energy is transmitted inside the reactor are conduction and convection.

3.2 Governing equations

The input for modelling (e.g., salt density, salt specific heat, conductivity and reaction enthalpy) is extracted from [2]. To predict the rates at which the chemical reactions take, equations 2 and 3 are solved for dehydration and hydration [2], respectively:

$$\frac{\partial X}{\partial t} = 1.38 \times 10^6 exp\left(\frac{E_a}{RT}\right) (1 - X) \left(1 - \frac{p}{p_{dhyd}}\right)^{1.79} \tag{2}$$

$$\frac{\partial X}{\partial t} = 3.04 \times 10^{-5} (1 - X) \left(T|_{P_{hyd}} - T \right)^{1.79} \tag{3}$$

where X represents the extent of reaction. E_a is activation energy, R is universal gas constant, T is the temperature and p is the pressure.

The effect of material porosity variation due to hydrate level over charging and discharging periods on transport phenomena and bed properties are reflected in modelling as below:

$$\varepsilon = \varepsilon_{ah} + h(\varepsilon_{mh} - \varepsilon_{ah}) \tag{4}$$

where h is the hydrate level. Also, ε_{ah} and ε_{mh} respectively refer to porosity of anhydrous and monohydrate salt.

The bed absorbs steam during hydration and desorb it during dehydration; hence, a mass source based on reaction kinetics is added to the mass conservation equation. The mass balance of porous medium is defined by:

$$\frac{\partial(\varepsilon\rho_g)}{\partial t} + \nabla \cdot \left(\rho_g \vec{v}\right) = \frac{dX}{dt} \varphi M_{H_2O} \tag{5}$$

where ρ_g is the density of gas, \vec{v} is the velocity vector of gas, φ is the volumetric molar number of salt contributing in the chemical reaction and M_{H_2O} molar mass of water.

To account for the effect of the porous mediums on the flow, Brinkman equations are implemented. The set of equations is linked with the source term of steam production/consumption. The momentum equation can be described by:

$$\frac{\rho_g}{\varepsilon} \frac{\partial(\vec{v})}{\partial t} + \frac{\rho_g}{\varepsilon} (\vec{v}. \nabla) \vec{v} \frac{1}{\varepsilon} =$$

$$\nabla \cdot \left[-pI + \frac{\mu}{\varepsilon} (\nabla \vec{v} + (\nabla \vec{v})^T) - \frac{2}{3} \frac{\mu}{\varepsilon} (\nabla \cdot \vec{v})I \right] - \left(\frac{\mu}{\kappa} + \beta \rho_g |\vec{v}| + \frac{dX}{dt} \varphi M_{H_2O} \right) \vec{v}$$
 (6)

here, μ is the dynamic viscosity, κ is the permeability of the porous medium, β is the inertial resistance coefficient based on Forchheimer parameter.

The energy balance within salt domain is expressed as follows:

$$\left(\rho C_{p}\right)_{eff} \frac{\partial T}{\partial t} + \rho_{g} C_{p,g}(\vec{v}.\nabla T) - \nabla \cdot \left(k_{eff} \nabla T\right) = -\frac{dX}{dt} \varphi \Delta H_{R}$$
(7)

where $(\rho C_p)_{eff}$ and k_{eff} are the effective volume heat capacity and the effective thermal conductivity, respectively.

To analyse the performance of the reactor, the thermal power consumption/generation by the chemical reaction at a specific time can be obtained based on the reaction rate (dX/dt):

$$P_x^t = \left(\frac{m_{SrBr_2}}{M_{SrBr_2}} \Delta H_R\right) \frac{dX}{dt} \tag{8}$$

where m_{SrBr_2} and M_{SrBr_2} are the mass and molar mass of material.

4. Results and discussion

This section delves into the primary results obtained using the model described in the previous section. The evaporator temperature is assumed to be at 170°C by solar thermal collector HTF and the condenser operates at 15°C. Furthermore, the HTF for hydration and dehydration enters the reactor at 300°C and 200°C, respectively. Under these conditions, steam with 792 kPa is generated for the hydration process which can potentially increase the salt temperature up to 331 °C based on figure 2.

The mass flow rate of HTF was set to 0.04 kg/s for each unit which consists of two symmetrical layers. The hydration level and temperature distribution inside one symmetrical layer at a specific time step of 1000s for both hydration and dehydration are displayed in Figure 4. For a specific reactor pressure, lower salt temperature leads to a higher driving force for hydration while a lower driving force for dehydration. Hence, for example for hydration, the regions inside material which is close either to the steam inlet or HTF channel have relatively lower temperatures and faster conversion.

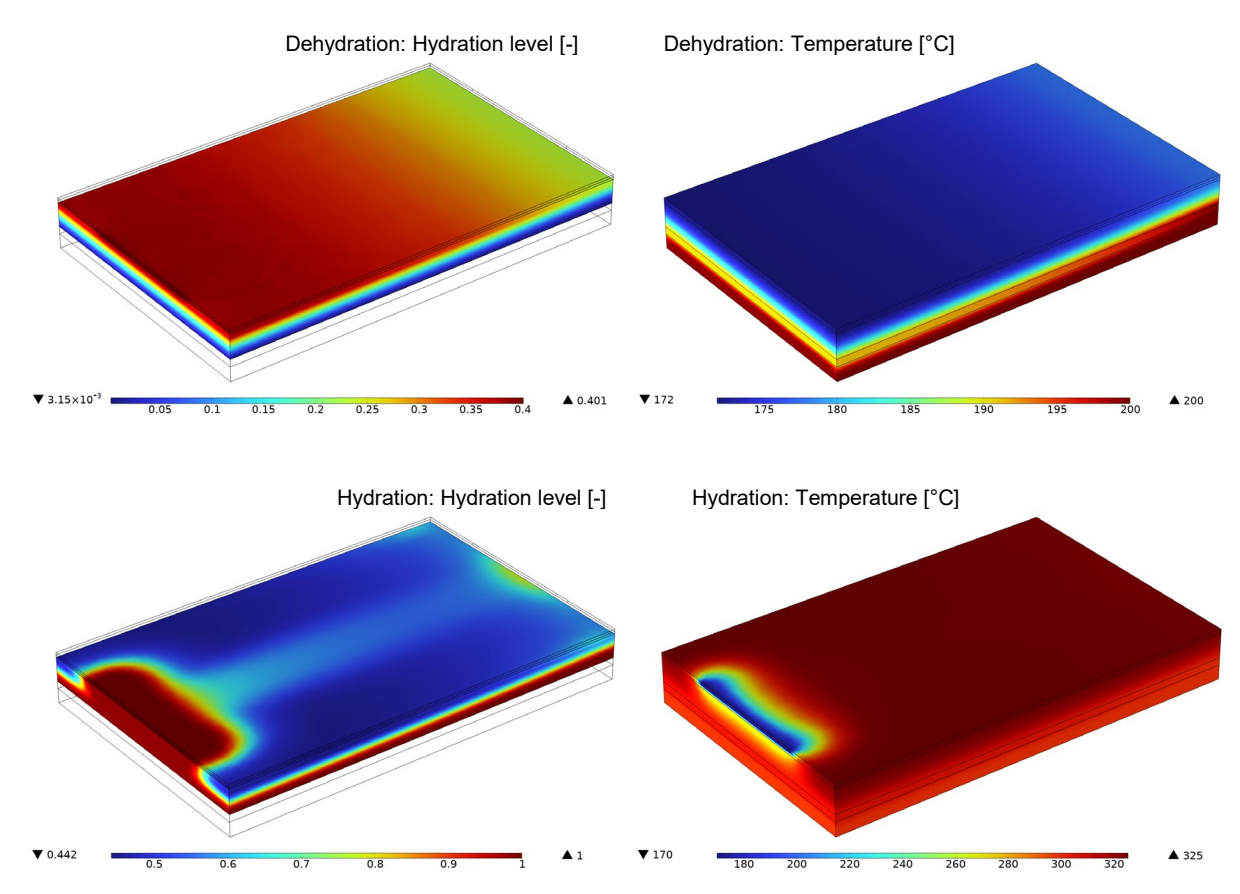


Figure 4. Hydration level inside the reactive material (SrBr₂) domain and temperature distribution inside the reactor at 1000s.

Figures 5 and 6 illustrate the system's behaviour over time during the charging phase. Once the reactor fully discharges, the endothermic reaction initiates. Figure 5 indicates that in the beginning, the conversion from monohydrate to anhydrous salt occurs quickly, resulting in a reduction of 37% within the first minute. Subsequently, the reaction rate gradually decreases, approaching completion after approximately 33 minutes. Figure 6 presents the variations in salt and HTF temperatures, along with power consumption. The salt temperature drops dramatically to a minimum of 175 °C because of the high rate of endothermic dehydration reaction, and then it experiences an increment reaching the HTF temperature. Likewise, power consumption starts at a peak value of 67.2 kW and decreases steeply. This initial spike is attributed to the high level of conversion driven by the strong driving force present when the material is first subjected to vacuum conditions.

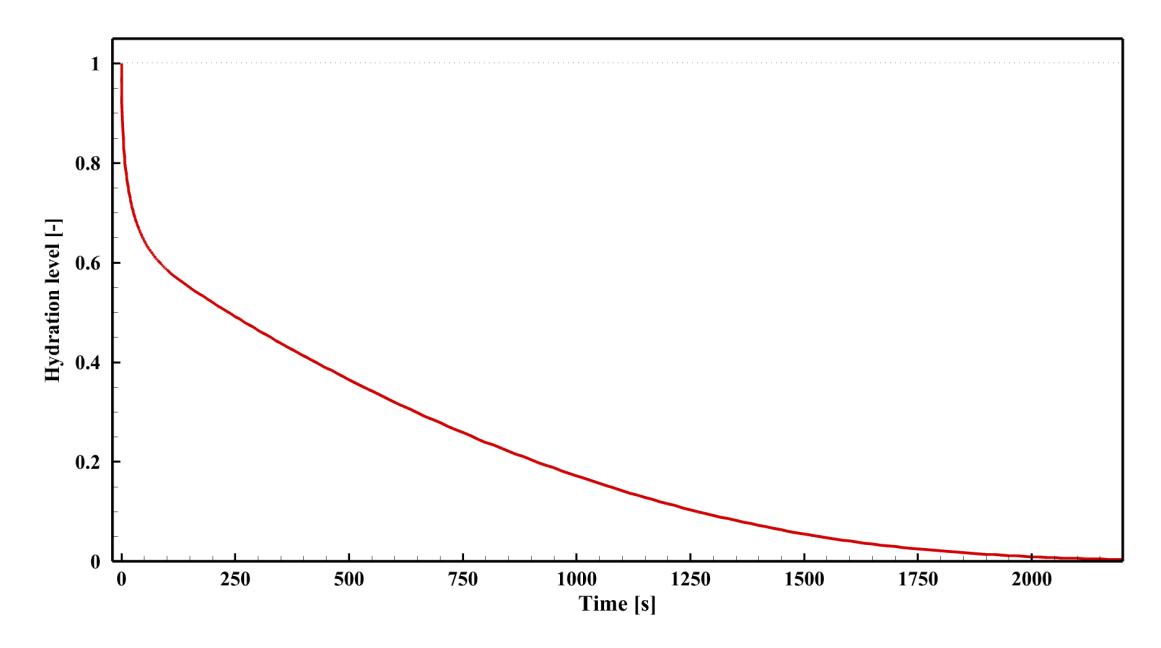


Figure 5. Hydration level during the charging period.

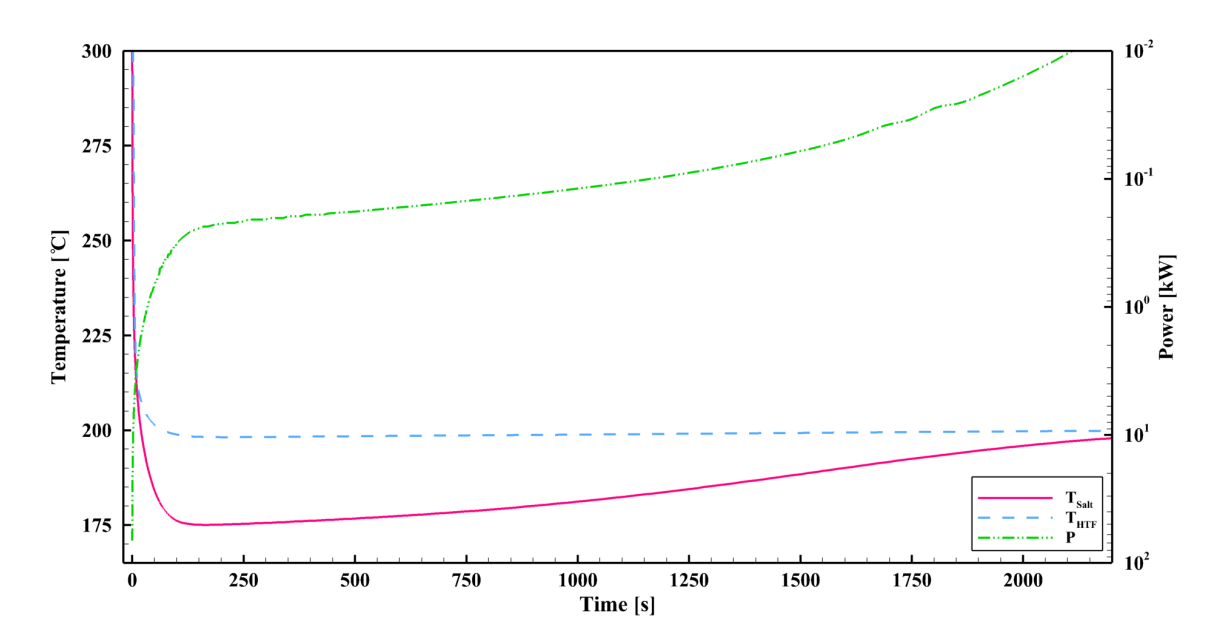


Figure 6. Variation of temperature along with power consumption during the charging period.

During the discharging process, the charged reactor acts in its exothermic mode. The trend of hydration level versus time is illustrated in Figure 7. According to equation 3, the lower salt temperature has a positive effect on the conversion rate. Once the evaporator valve opens and the reaction starts, the conversion occurs fast due to the high reaction rate; however, as the reactive material temperature rises, the reaction rate decreases because the temperature reaches close to the equilibrium temperature and the conversion slope falls continuously. The results shown in Figure 8 indicate that the material temperature rises sharply, peaking at 322.5 °C after 130s, followed by a decline, reaching 300 °C after approximately 40 minutes. Furthermore, the power generated by the chemical reaction starts with a peak value of 72.1 kW and decreases sharply, similar to the dehydration process.

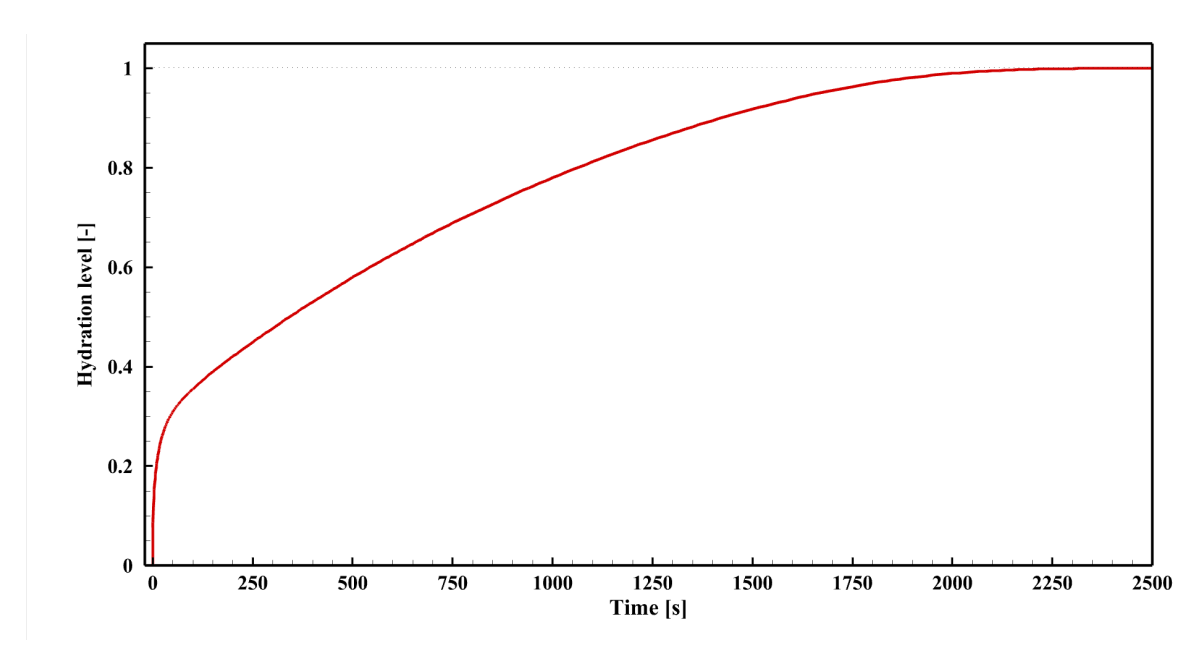


Figure 7. Hydration level during the discharging period.

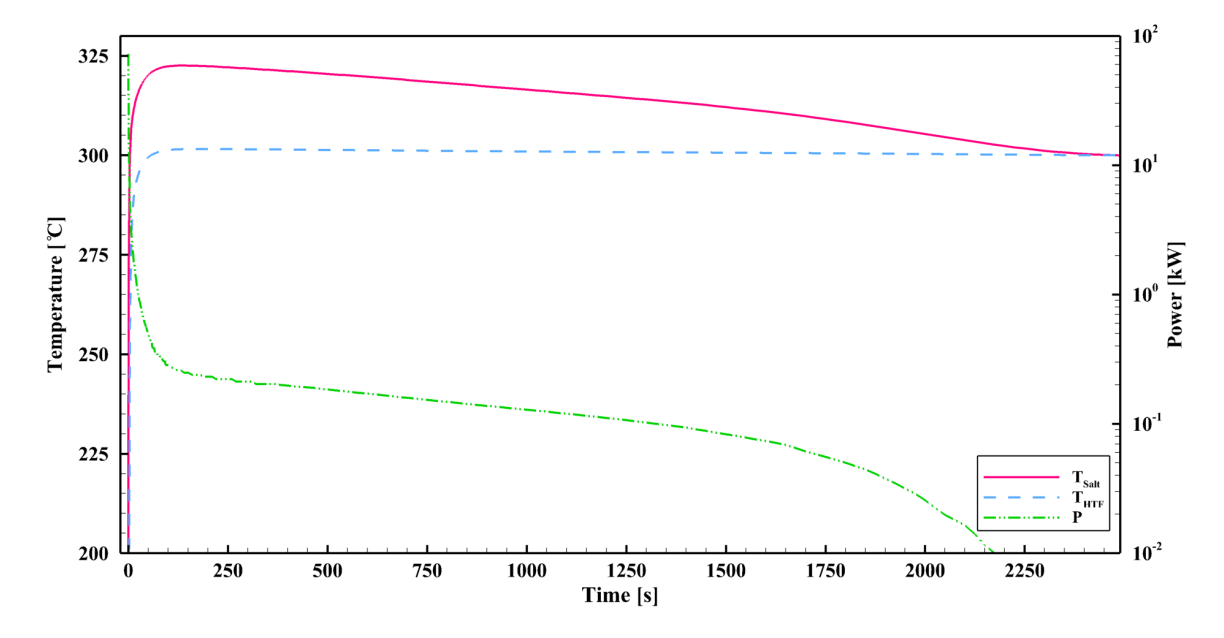


Figure 8. Variation of temperature along with power consumption during the discharging period.

These results show the potential of this heat transformer for upgrading the heat from the solar collectors and making it suitable for various industrial processes. Depending on the availability of solar radiation and the waste heat temperature, different operating conditions can be achieved for heating purposes, which opens up possibilities for various industrial heating applications.

5. Conclusion and outlook

The objective of this research was to investigate a novel design of a solar thermochemical heat transformer suitable for industrial heating applications. It is based on a packed bed of particles (SrBr₂) in which heat is transferred indirectly to the heat transfer fluid. It has a compact design, no moving components, and relatively low construction cost, making it suitable for several applications. A numerical model comprising heat and mass transfer coupled with the chemical

kinetics was developed to assess the performance. The evaporator and condenser temperatures are assumed to be at 170°C and 15°C, respectively. The inlet HTF temperature for hydration and dehydration processes are assumed to be at 300°C and 200°C, respectively. A complete conversion is predicted by the numerical model during the charging process. Based on the thermodynamics of the reactive system, 331 °C temperature is expected to be achieved during the discharging process. The model predicts achieving 322.5 °C temperature which shows the efficiency of the proposed reactor. The proposed design can potentially upgrade the temperature by 100 °C and maintain it at 300 °C for about 40 minutes. The heat effect is clearly visible during the discharging process. In the future, this model will be used to optimize the reactor geometry and validated against the experimental results.

Data availability statement

Data will be made available on request.

Author contributions

Ramin Roushenas: Conceptualization, Investigation, Software, Formal analysis, Methodology, Visualization, Writing-original draft; Marco Ballatore: Conceptualization, Investigation; Artem Sybir: Conceptualization, Writing-review & editing, Funding acquisition; Aldo Cosquillo: Conceptualization, Writing-review & editing, Funding acquisition; Marc Linder: Conceptualization, Writing-review & editing, Funding acquisition; Abhishek K. Singh: Conceptualization, Supervision, Methodology, Writing-review & editing, Funding acquisition

Competing interests

The authors declare that they have no competing interests.

Funding

This work was performed within Project "TechUPGRADE: Thermochemical Heat Recovery and Upgrade for Industrial Processes" that have received funding from the European Commission, through the HORIZON EUROPE, RIA – Research and Innovation Actions programmes under grant agreement No 101103966.

References

- [1] Roushenas R, Rahbari HR, Alsagri AS, Arabkoohsar A. Improved marketing strategy of a hybrid renewable plant integrated with gravitational energy storage: Techno-economic analysis and multi-objective optimization. J Energy Storage 2024;78. https://doi.org/10.1016/j.est.2023.109991.
- [2] Stengler J, Bürger I, Linder M. Performance analysis of a gas-solid thermochemical energy storage using numerical and experimental methods. Int J Heat Mass Transf 2021;167. https://doi.org/10.1016/j.ijheatmasstransfer.2020.120797.
- [3] Rui J, Luo Y, Wang M, Peng J, She X. Design and performance evaluation of an innovative salt hydrates-based reactor for thermochemical energy storage. J Energy Storage 2022;55. https://doi.org/10.1016/j.est.2022.105799.
- [4] Humbert G, Sciacovelli A. Design of effective heat transfer structures for performance maximization of a closed thermochemical energy storage reactor through topology optimization. Appl Therm Eng 2024;239. https://doi.org/10.1016/j.applthermaleng.2023.122146.
- [5] Stengler J, Bürger I, Linder M. Thermodynamic and kinetic investigations of the SrBr2 hydration and dehydration reactions for thermochemical energy storage and heat transformation. Appl Energy 2020;277. https://doi.org/10.1016/j.apenergy.2020.115432.